Purdue University
Purdue e-Pubs

International Compressor Engineering Conference

School of Mechanical Engineering

2000

Mixed Lubrication Analysis of Vane Tip in Rotary Compressor

S. Tanaka
Tokyo Institute of Technology

T. Nakahara
Tokyo Institute of Technology

K. Kyogoku
Tokyo Institute of Technology

MIXED LUBRICATION ANALYSIS OF VANE TIP IN ROTARY COMPRESSOR

Shinji TANAKA, Tsunamitsu NAKAHARA and Keiji KYOGOKU
Department of Mechanical and Intelligent Systems Engineering
Tokyo Institute of Technology
2-12-1, O-okayama, Meguro-ku, Tokyo 152-8552, JAPAN

ABSTRACT

This paper shows the mixed lubrication analysis between the vane tip and rolling piston in a rotary refrigerant compressor, coupling the motion equations of vane and rolling piston, the elastohydrodynamic lubrication (EHL) analysis of line contact and the equations of viscosity characteristics of lubricating oil as a function of oil pressure, oil temperature and concentration of refrigerant. The p_cV value, that is, the product of solid contact pressure by sliding speed between vane tip and rolling piston, has been calculated. The calculations have been made for various operation conditions and viscosity grades of oil.

NOMENCLATURE

a: thickness of vane, m
b: half Hertzian length ($=R(8w/\pi)^{0.5}$), m
C: constant
C_p: specific heat of vane and piston, 480 J/(kg·K)
E: equivalent Young's module of vane and piston, 165 GPa
e: eccentricity ($=R_c - r_o$), m
F_{ct}: viscosity resistance between piston and cylinder, N
F_{n1}, F_{n2}: normal force between vane and cylinder slot, N
F_s: spring force, N
F_{t1}, F_{t2}: friction force ($=\mu_s F_{n1}$, $\mu_s F_{n2}$), N
F_v: viscosity friction force of vane end face, N
F_{vn}: load of vane tip, N
F_{vt}: friction force of vane tip, N
F_{vx}, F_{vy}: gas force in direction of x, y axes acting on vane, N
h: nominal oil film thickness, m
h_0: central oil film thickness, m
h_t: average oil film thickness, m
I_p: inertial moment of piston, N·m
K_{f0}: thermal conductivity of lubricant, 0.125 W/(m·K)
K_p: thermal conductivity of vane and piston, 38 W/(m·K)
k_c: constant
l_p: length of piston, m
l_s: length of cylinder slot, m
M_c: moment of viscosity friction between rolling piston and shaft, N·m
M_p: moment of viscosity friction of piston end face, N·m
M_v: rotational moment acting on vane, N·m
m_0: viscosity-temperature property from the ASTM-Walther equation (=ASTM slope/0.2)
m_v: mass of vane, kg
O: center point of cylinder
O_p: center point of eccentric shaft
p_c: solid contact pressure, Pa
p_{com}: compression chamber pressure, Pa
p_d: discharge pressure, Pa
p_f: oil film pressure, Pa
p_{suc}: suction pressure, Pa
R: equivalent curvature radius between vane and rolling piston ($1/R=1/r_o+1/r_v$), m
R_c: radius of cylinder, m
r: constant
r_i: inner radius of piston, m
r_o: outer radius of piston, m
r_v: radius of vane tip, m
S: non dimensional average shear stress
t: time
u: entrainment velocity ($=\Delta u/2+r_v\dot{\alpha}$), m/s
v: relative velocity ($=r_o\omega_p+(r_o+r_v)\dot{\alpha}$), m/s
w: load of vane tip per unit of width ($=F_{vn}/l_p$), N/m
x: coordinate, m
x_e: location where oil film breaks, m
x_{end}: outlet location, m
x_{min}: inlet location, m
x_v: displacement of vane ($=(r_v+r_o)\cos\alpha+e\cos\theta$), m
α: attitude angle of rolling piston, rad
α_0: viscosity-pressure coefficient, Pa^{-1}
β: viscosity-temperature coefficient, 0.025 ℃$^{-1}$
ΔT: temperature rise of lubricant, ℃
ΔT_c: temperature rise caused by solid contact, ℃
ΔT_f: temperature rise at parallel area, ℃
ΔT_{in}: temperature rise at intake area, ℃
Δu: sliding velocity at vane tip contact ($=r_o\omega_p$), m/s
δ: elastic deformation, m
η: viscosity of oil dissolving refrigerant, Pa·s
η_0: viscosity of oil dissolving refrigerant at atmospheric pressure, Pa·s
θ: rotational angle of shaft, rad
μ: coefficient of boundary friction

μ_0: kinematic viscosity of oil dissolving refrigerant, m^2/s
μ_s: coefficient of friction between vane and cylinder
ρ: density of oil dissolving refrigerant, kg/m^3
ρ_p: density of vane and rolling piston, 7800 kg/m^3
Σ_i: non dimensional equivalent isothermal shearing velocity
σ: composite RMS roughness of vane and rolling piston, m
τ_0: specific shear stress, Pa
τ_c: average shear stress due to solid contact, Pa
τ_f: average shear stress of fluid, Pa
Φ: non dimensional temperature rise
ϕ_x: pressure flow factor
χ: coefficient of temperature rise due to shear
ω_p: angular velocity of piston, rad/s

INTRODUCTION

A rolling piston type rotary refrigerant compressor is widely used for refrigerator and air conditioner. The contact between vane tip and rolling piston is under the most severe lubricated condition in this compressor, and the sliding speed is dependent on the frictions between the vane tip and the piston and between the piston and eccentric shaft because the rolling piston freely rotates the circumference of eccentric shaft. In addition, there exists the moment when the entrainment velocity which causes the hydrodynamic lubrication action becomes zero due to peculiar motion to a cam. Moreover, the refrigerating machine oil dissolves much refrigerant gas so that the viscosity is greatly reduced and thus it is difficult to form the fluid film. Therefore, the lubrication of vane tip contact significantly influences the performance and reliability of the compressor.

Although it is necessary to evaluate exactly such severe lubrication condition as mentioned above, there are few reports on unsteady mixed lubrication analysis of the vane tip considering EHL [1]. The authors have shown the mixed lubrication analysis method of vane tip in a rotary compressor [2].

This paper shows the results of the dynamic simulation of the mixed lubrication characteristics between the vane tip and the rolling piston under the lubrication with refrigerating machine oil dissolving hydrofluorocarbon (HFC) refrigerant.

ANALYSIS METHOD

Figure 1 shows an analytical model of a rolling piston type rotary compressor. It is considered that the contact conditions between the surface of vane side and the cylinder slot vary with the shaft angle. However, to calculate easily, it is assumed in this paper that the vane always leans as shown in Figure 1.

Viscosity Characteristics of Lubricants Dissolving Refrigerant

To obtain the viscosity-pressure coefficient α_0 of lubricating oil dissolving refrigerant, the So and Klaus's experimental formula [3] which is widely used for mineral oil is expanded for the lubricant dissolving refrigerant.

$$a_0 = 1.030 + 3.509(\log\mu_0)^{3.0627} + 2.412\times10^{-4} m_0^{5.1903}(\log\mu_0)^{1.5976} - 3.387(\log\mu_0)^{3.0975}\rho_0^{0.1162} \quad (1)$$

The viscosity-pressure-temperature property are obtained from the following equation including Barus's formula.

$$\eta = \eta_0 \exp(a_0 p - \beta\Delta T) \quad (2)$$

The lubricating oil used in this paper is polyol ester (POE) and the refrigerant is HFC-134a. The viscosity-pressure property calculated under the above assumption at 40 ℃ is shown in Figure 2.

Motion Equations of Vane and Rolling Piston

The equations integrated theoretical equations of Yanagisawa [4], Imaichi et al. [5], Sakurai and Hamilton [6] are used for the motion equations of the vane and the rolling piston. The load of vane tip F_{vn} is obtained by equilibrating the forces and moments of vane in the directions of the x and y axes.

$$m_v\ddot{x}_v = F_{vx} + F_{t1} + F_{t2} + F_{vn}\cos a + F_{vt}\sin a - F_s + F_v \quad (3)$$

$$F_{vy} + F_{n1} - F_{n2} + F_{vt}\cos a - F_{vn}\sin a = 0 \quad (4)$$

$$(R_c+l_s-x_v)F_{n1}+\frac{a}{2}F_{t1}-(R_c-x_v)F_{n2}-\frac{a}{2}F_{t2}+M_v-r_vF_{vt}=0 \tag{5}$$

The rotational motion equation of the rolling piston is shown as follows:

$$I_p\dot{\omega}_p=M_c-M_p-r_o(F_{vt}+F_{ct}) \tag{6}$$

Mixed Lubrication Analysis

The partial EHL analysis method that has been shown by Nakahara et al. [7] is used. The assumptions and basic equations are shown as follows:

(1) The vane tip is in line contact. In other words, the pressure of oil film and the elastic deformation distribute one dimensional.

(2) The surface roughness is parallel to the direction of sliding.

$$\phi_x=1+C(\tfrac{h}{\sigma})^{-r} \tag{7}$$

(3) The Reynolds equation modified by Patir and Cheng [8] taking surface roughness into consideration is applied for the pressure equation of oil film. The Swift-Stieber (Reynolds) condition is used for the boundary condition.

$$\frac{\partial}{\partial x}\left(\phi_x\frac{\rho h^3}{\eta}\frac{\partial p_f}{\partial x}\right)=12u\frac{\partial \rho h_t}{\partial x}+12\frac{\partial \rho h_t}{\partial t} \tag{8}$$

(4) The elastic deformation on the surface is expressed as

$$\delta=-\frac{2}{\pi E}\int_{x_{\min}}^{x_e}p_f\ln(x-x')^2dx'-\frac{2}{\pi E}\int_{x_{\min}}^{x_{end}}p_c\ln(x-x')^2dx' \tag{9}$$

Then, the oil film thickness is given as

$$h=h_0+\frac{x^2}{2R}+\delta(x)-\delta(0) \tag{10}$$

(5) It is assumed that the relationship between the film thickness h and the average film thickness h_t is the same as the Gaussian distribution.

$$h_t=\frac{h}{2}\left\{1+\mathrm{erf}\left(\frac{h}{\sqrt{2}\,\sigma}\right)\right\}+\frac{\sigma}{\sqrt{2\pi}}\exp\left(-\frac{h^2}{2\sigma^2}\right) \tag{11}$$

(6) The experimental expression of the density-pressure relationship is

$$\rho=\rho_0\left(1+\frac{0.6\times10^{-9}p_f}{1+1.7\times10^{-9}p_f}\right) \tag{12}$$

(7) The contact pressure is calculated from the approximative equation of Patir and Cheng [9] which is based on the theory developed by Greenwood and Tripp [10].

$$p_c=\begin{cases}4.4086\times10^{-5}k_cE(4-\frac{h}{\sigma})^{6.804} & (h<4\sigma)\\ 0 & (h\geqq 4\sigma)\end{cases} \tag{13}$$

(8) The average shear stress of oil film is calculated from following equations [11].

$$\tau_f=S\tau_0 b \tag{14}$$

$$S=\frac{\ln(2\Sigma_i)}{1+\Phi\Sigma_i} \tag{15}$$

(9) The friction force due to solid contact is calculated as follows:

$$\tau_c=\mu p_c \tag{16}$$

(10) It is assumed that the temperature rise of fluid due to the friction is the sum of following temperature rises.

(i) Temperature rise due to shear heat at the intake area [12]:

$$\Delta T_{in}=\frac{\eta_0u^2}{5K_{f0}} \tag{17}$$

(ii) Temperature rise due to shear heat at the parallel area [13]:

$$\Delta T_f=\chi\tau_f\Delta u \tag{18}$$

(iii) Flash temperature due to solid contact [14]:

$$\Delta T_c=0.752\mu p_c\sqrt{\frac{\Delta ub}{2K_p\rho_pC_p}} \tag{19}$$

Procedure of Calculation

To obtain the oil film thickness h and the oil film pressure p_f, the EHL analysis linking equations (2), (7)-(12) is simultaneously solved using the Newton-Raphson method. The solid contact pressure p_c is calculated from h and equation (13), and the calculation is repeated until p_c and p_f are satisfied with the following equation of load balance.

$$w=\int_{x_{\min}}^{x_e}p_fdx+\int_{x_{\min}}^{x_{end}}p_cdx \tag{20}$$

Then the temperature rise of oil film and the friction force is calculated from equations (14)-(19).

The above calculations are simultaneously solved coupling the motion equations (3)-(6) and the equations of viscosity of lubricating oil varying due to pressure and concentration of refrigerant.

RESULTS AND DISCUSSION

Table 1 shows the dimensions of the compressor as a object of the analysis which is a standard refrigerant compressor for home-use air conditioners. Table 2 shows the standard operating condition in the numerical simulations. The temperature 40 ℃, which is equal to the temperature of the discharge gas, is selected as a representative temperature of lubricant in the compressor. In this analysis, the friction coefficients at solid contact are assumed as follows [15]:

Coefficient of boundary friction $\mu = 0.118$

Friction coefficient at vane side contacts $\mu_s = 0.100$

Figure 3 shows the load of vane tip per unit of width under the standard condition. The load increases suddenly at 0 degree and 180 degree in the shaft angle because the direction of friction force between the vane and the cylinder reverses at these shaft angles. In addition, the great increase in load is due to the assumption of the friction coefficient of vane side surface μ_s to be 0.1. The entrainment, sliding and relative velocities of the vane tip are indicated in Figure 4 for the standard condition as well. The entrainment velocity means the velocity pulling the lubricant into the wedge between the contact surfaces, the sliding velocity is the relative velocity at the contact point between vane tip and the rolling piston and the relative velocity means the sliding velocity plus the motion velocity of the contact point. Since the entrainment velocity goes to zero as the shaft angle approaches 90 degree and 270 degree, the lubricating condition of vane tip becomes particularly severe at these shaft angles.

Figure 5 presents the variation of p_cV value under the standard condition. The p_cV value represents the multiplying the solid contact pressure of vane tip by the sliding velocity at vane tip contact. The p_cV value indicates the highest value in one rotation of the shaft at 307 degree in the shaft angle. The p_cV value becomes zero around 90 degree in the shaft angle because the sliding velocity is zero at this shaft angle.

The effect of the viscosity grade of oil on the p_cV value of vane tip is demonstrated in Figure 6. The peak of p_cV value increases with an increase in viscosity grade of oil because the sliding velocity at vane tip contact increases as indicated in Figure 7. However, the p_cV value around 180 degree in the shaft angle decreases with an increase in viscosity grade of oil because of the increase in oil film thickness with increasing the viscosity of oil.

Figure 8 shows the effect of the viscosity grade of oil on the friction loss by solid contact and the viscous friction loss of oil at vane tip contact. The friction loss by solid contact is not influenced by the viscosity grade of oil, but the viscous friction loss increases as the viscosity grade increases.

The effect of rotational speed of the shaft on the p_cV value are demonstrated in Figure 9. As the rotational speed of the shaft increases, the peak of the p_cV value increases. This reason is that the sliding velocity at vane tip contact increases more than the load decreases with an increase in rotational speed of shaft as shown in Figure 10, although the peak load of vane tip at the shaft angle of 180 degree decreases with an increase in rotational speed of shaft due to the inertia of vane as shown in Figure 11.

Figure 12 shows the effect of rotational speed of the shaft on the friction losses at the vane tip contact. Both friction losses increase with an increase in rotational speed of the shaft because the sliding velocity at vane tip contact increases.

As the rotational speed of shaft increases, the oil temperature in a compressor tends to rise. The effect of the temperature rise of oil on the friction losses of vane tip at 5,400 rpm is shown in Figure 13. The viscous friction loss of fluid film is the highest at 60 ℃ because the oil viscosity and the sliding velocity at vane tip contact at 60 ℃ is the highest as shown in Table 3 and Figure 14, respectively. On the contrary, the friction loss by solid contact is the lowest at 60 ℃.

CONCLUDING REMARKS

The lubrication characteristics of the vane tip in a rotary compressor has been demonstrated by using the mixed lubrication analysis that has solved simultaneously the elastohydrodynamic lubrication equations, the contact ones and the motion ones of a vane and a rolling piston.

The results indicate that the viscosity of oil which is influenced by dissolving concentration of refrigerant as well as temperature affects the p_cV value and the friction loss by solid contact and the viscous friction loss of fluid significantly.

REFERENCES

[1] Yoshimura, T., Ono, K., Inagaki, K., Kotsuka, H. and Korenaga, A., "Analysis of Lubricating Characteristics in Rotary Compressors for Domestic Refrigerators," *Transactions of the Japan Society of Mechanical Engineers (in Japanese)*, Series C, Vol.63, No.615, 1997, pp.4004-4011.

[2] Tanaka, S., Kyogoku, K. and Nakahara, T., "Lubrication Characteristics of Refrigerating / Air Conditioning Rotary Compressor : Mixed Lubrication Analysis on Vane Tip," *Journal of Japanese Society of Tribologists (in Japanese)*, Vol.41, No.3, 1996, pp.247-254.

[3] So, B. Y. C. and Klaus, E. E., "Viscosity-Pressure Correlation of Liquids," *ASLE Transactions*, Vol.23, No.4, 1980, pp.409-421.

[4] Yanagisawa, T., *Transactions of the Japan Society of Mechanical Engineers (in Japanese)*, Series C, Vol.48, No.429, 1982, pp.732-740.

[5] Imaichi, K., Fukushima, M., Muramatsu, S. and Ishii, N., *Transactions of the Japan Society of Mechanical Engineers (in Japanese)*, Series C, Vol.49, No.447, 1983, pp.1959-1970.

[6] Sakurai, E. and Hamilton, J. F., "The Prediction of Frictional Losses in Variable-Speed Rotary Compressors," *Proceedings of the 1984 International Compressor Engineering Conference at Purdue*, 1984, pp.331-338.

[7] Nakahara, T., Yamaji, M. and Kyogoku, K., *Proceedings of JAST Tribology Conference Morioka (in Japanese)*, 1992, pp.703-706.

[8] Patir, N. and Cheng, H. S., "An Average Flow Model for Determining Effects of Three-Dimensional Roughness on Partial Hydrodynamic Lubrication," *Transactions of ASME:Journal of Lubrication Technology*, Vol.100, 1978, pp.12-17.

[9] Patir, N. and Cheng, H. S., "Effect of Surface Roughness Orientation on The Central Film Thickness in E.H.D. Contacts," *Proceedings of the 5th Leeds-Lyon Symposium on Tribology*, 1978, pp.15-21.

[10] Greenwood, J. A. and Tripp, J. H., "The Contact of Two Nominally Flat Rough Surfaces," *Proceedings of the Institution of Mechanical Engineers*, Vol.185, 1970-71, pp.625-633.

[11] Muraki, M. and Kimura, Y., "Calculation of EHL Traction with Low-Viscosity Fluids by Using an Eyring Viscous Solution," *Transactions of the Japan Society of Mechanical Engineers (in Japanese)*, Series C, Vol.55, No.520, 1989, pp.3048-3055.

[12] Muraki, M. and Kimura, Y., "Influence of Temperature Rise on Shear Behaviour of an EHL Oil Film," *Transactions of the Japan Society of Mechanical Engineers (in Japanese)*, Series C, Vol.56, No.528, 1990, pp.2226-2234.

[13] Muraki, M. and Kimura, Y., "Traction Characteristics of Lubricating Oils (2nd Report)," *Journal of Japanese Society of Lubrication Engineers (in Japanese)*, Vol.28, No.10, pp.753-760.

[14] Jaeger, J. C., "Moving Sources of Heat and the Temperature at Sliding Contacts", *Journal and Proceedings of the Royal Society of New South Wales*, Vol.76, 1942, pp.203-224.

[15] Tanaka, S., Momozono, S., Kyogoku, K. and Nakahara, T., "Estimation of Coefficient of Boundary Friction under Mixed Lubrication in Refrigerant Atmosphere," *Journal of Japanese Society of Tribologists (in Japanese)*, Vol.44, No.5, 1999, pp.358-365.

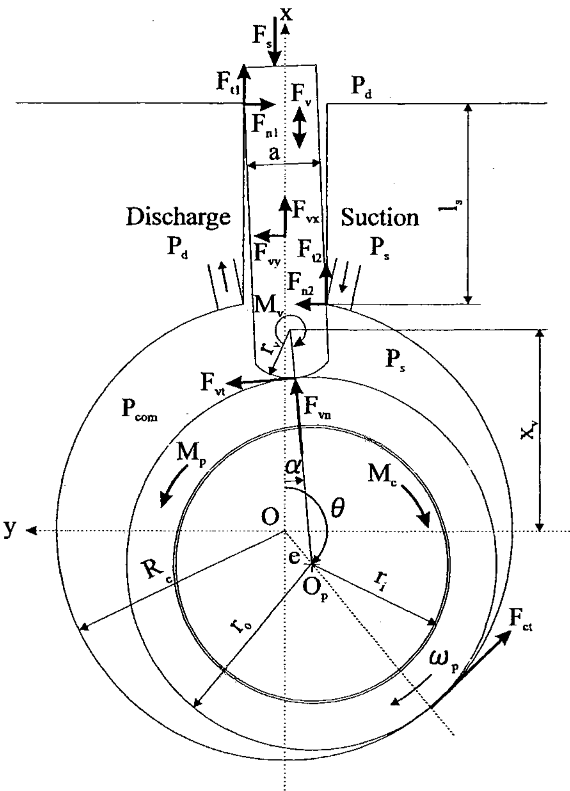

Fig. 1 Analytical model

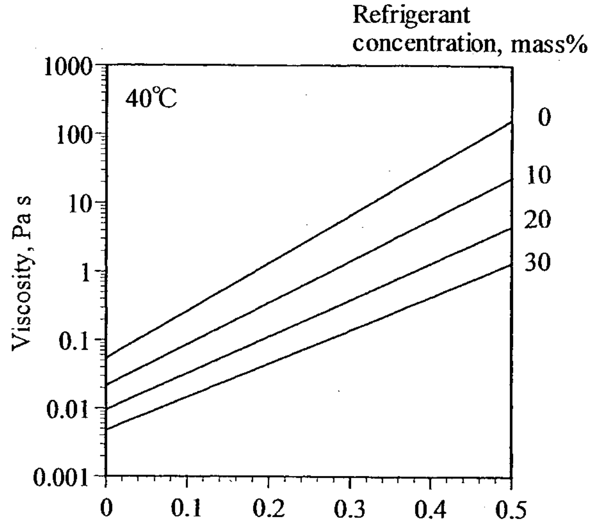

Fig. 2 Viscosity-pressure property of HFC-134a / POE(VG56)

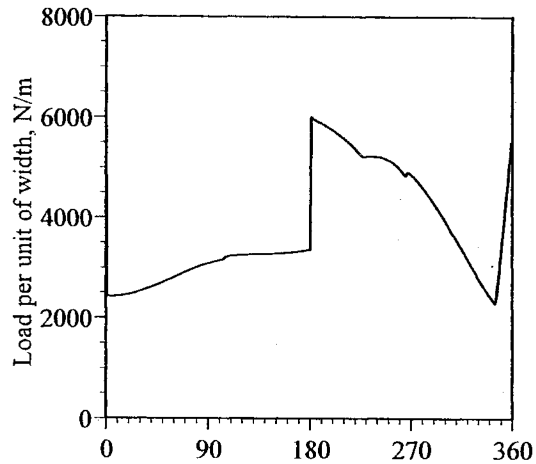

Fig. 3 Load of vane tip per unit of width

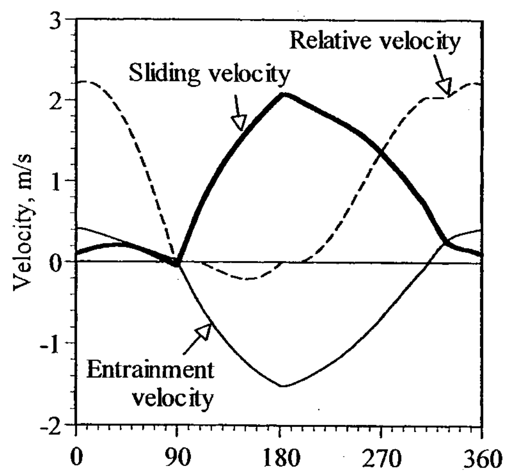

Fig. 4 Velocities of vane tip

Table 1 Dimensions of compressor

Radius of cylinder R_c, m	22.0×10^{-3}
Outer radius of piston r_o, m	17.8×10^{-3}
Inner radius of piston r_i, m	13.35×10^{-3}
Length of piston l_p, m	25.0×10^{-3}
Radius of vane tip r_v, m	6.3×10^{-3}
Thickness of vane a, m	4.0×10^{-3}
Composite RMS roughness σ, m	0.1×10^{-6}
Mass of vane m_v, kg	16.5×10^{-3}
Mass of piston, kg	84.9×10^{-3}

Table 2 Standard condition in simulation

Rotational speed of shaft, rpm	3,600
Discharge pressure p_d, Pa	1.02×10^{6}
Suction pressure p_{suc}, Pa	0.09×10^{6}
Refrigerant concentration, mass%	22.3
Temperature of oil, ℃	40
Viscosity grade of oil	VG56

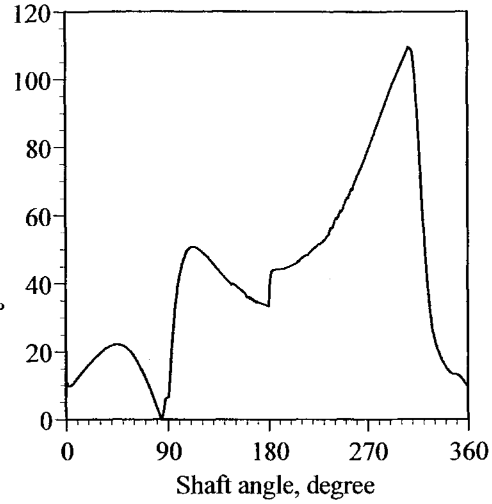

Fig. 5 p_cV value of vane tip

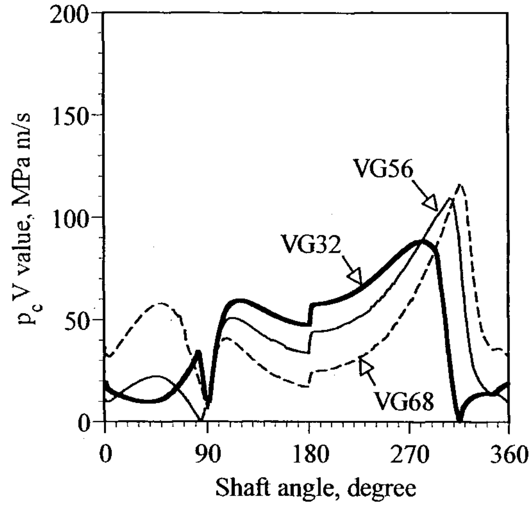

Fig. 6 Effect of viscosity grade on p_cV value

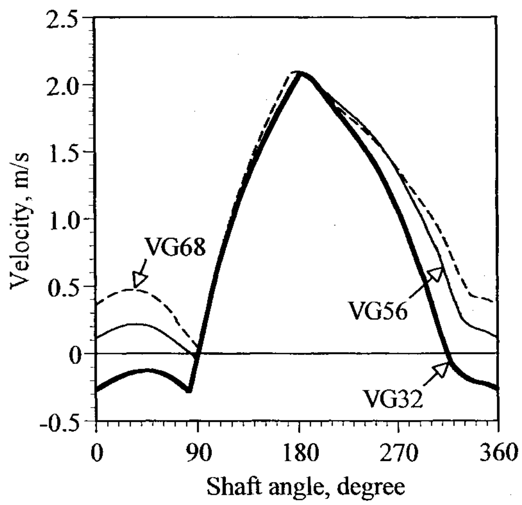

Fig. 7 Effect of viscosity grade on sliding velocity

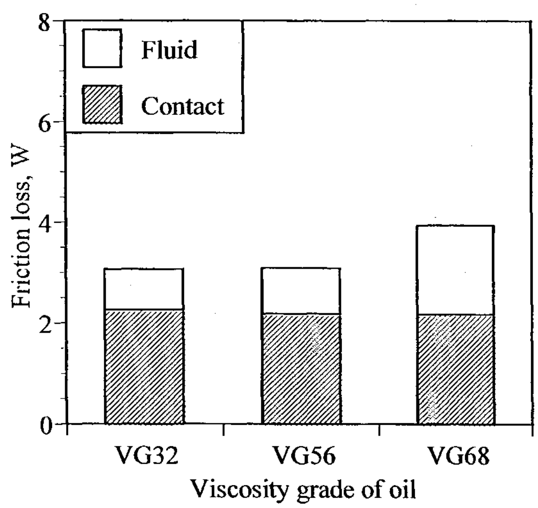

Fig. 8 Effect of viscosity grade on friction loss

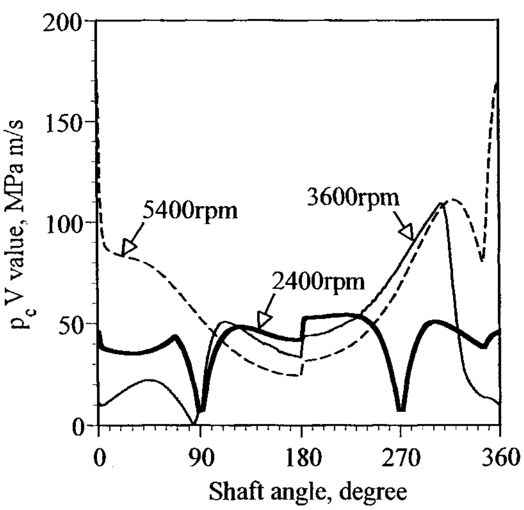

Fig. 9 Effect of rotational speed of shaft on p_cV value

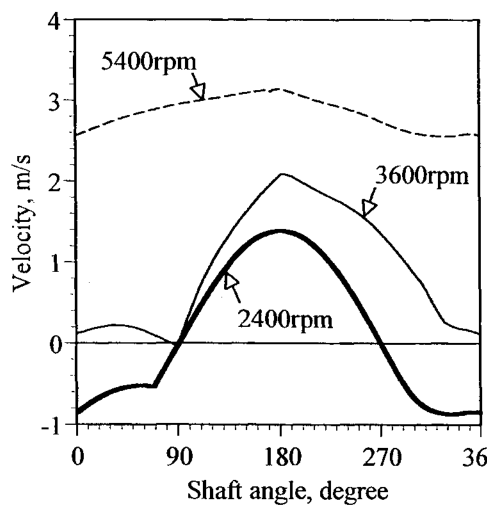

Fig. 10 Effect of rotational speed of shaft on sliding velocity

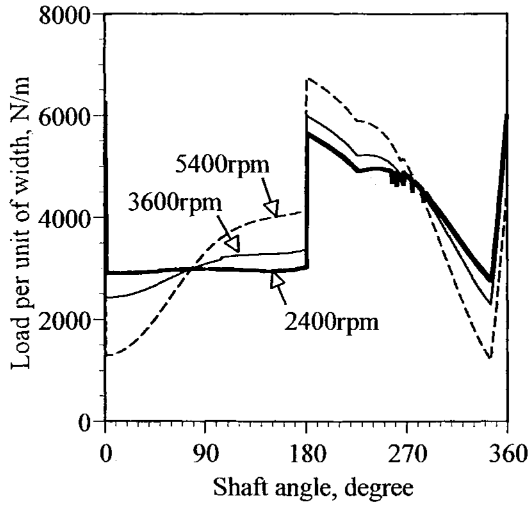

Fig. 11 Effect of rotational speed of shaft on load of vane tip

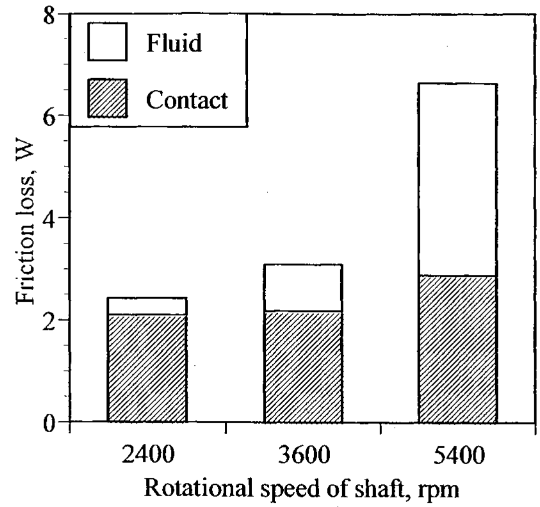

Fig. 12 Effect of rotational speed of shaft on friction loss

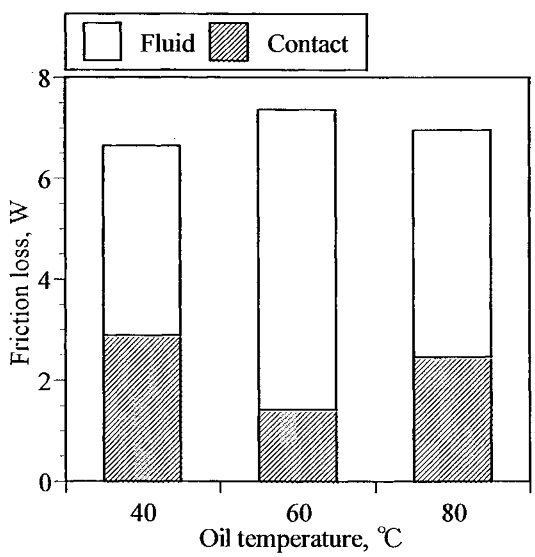

Fig. 13 Effect of oil temperature on friction loss

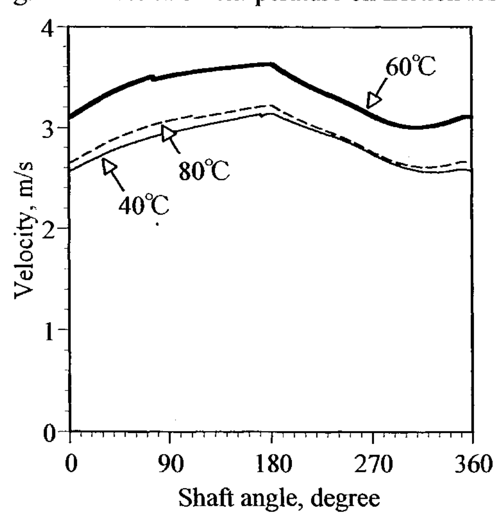

Fig. 14 Effect of oil temperature on sliding velocity

Table 3 Refrigerant concentration and oil viscosity

Oil temperature, ℃	Refrigerant concentration, mass%	Oil viscosity, Pa·s
40	22.3	7.5×10^{-3}
60	11.0	9.3×10^{-3}
80	5.3	7.9×10^{-3}